https://doi.org/10.1016/j.combustflame.2017.10.040

Circulation-controlled firewhirls with differential diffusion

Dehai Yu and Peng Zhang*

Department of Mechanical Engineering, the Hong Kong Polytechnic University,

Hung Hom, Kowloon, Hong Kong

Abstract

A flame-sheet theory for circulation-controlled firewhirls with differential diffusion is presented to investigate the effects of non-unity and unequal Lewis numbers on the flame shape and height of the firewhirls. Variable physical properties and a piecewise generalized power-law vortex model are implemented in the theory. For the fuel and oxidizer Lewis numbers being unequal but close to unity, the perturbation solutions of the Burke-Schumann-like transport equation for the Lewis-number-weighted coupling functions were obtained by using the Green's function method. The derived flame height expression not only confirms the previous discoveries, such as the Peclet number effect found by Chuah *et al*. (2011), the strong vortex effect by Klimenko and William (2013), and the variable density and mass diffusivity effects by Yu and Zhang (2017), but also demonstrates that the mass-diffusivity-ratio model correction newly proposed by Yu and Zhang (2017) is attributable to the leading-order non-unity Lewis number effect. The validity of the differential diffusion effects on the flame height was extended to arbitrary Lewis numbers and verified by means of the approximate far-field similarity solutions of the mixture fraction.

Keywords: Firewhirl, Differential diffusion, Non-unity Lewis number, Perturbation theory, Green's function, Far-field similarity solution

* Corresponding author
E-mail: pengzhang.zhang@polyu.edu.hk
Fax: (852)23654703 Tel: (852)27666664

1. Introduction

Firewhirls are destructive natural phenomena that can be characterized as open diffusion flames intensified by strong vortices formed under suitable terrain and meteorological conditions [1-5]. Numerous theoretical and laboratory investigations have been carried out in the past for understanding the occurrence, mechanisms and behaviors of firewhirls [1-20]. Although buoyancy effects are considered generally indispensable to firewhirls, circulation-controlled firewhirls were found in nature [2, 21, 22] and reproduced in laboratory by Chuah *et al*. [3], who observed a sufficiently strong, inclined vortical flow generated a correspondingly oriented firewhirl over a liquid fuel containing pan, thus testifying the dominance of circulation over buoyance. To explain the experimental observation, they established a steady-state, axisymmetric, diffusion flame-sheet theory with the following major approximations:

1. the firewhirl has a large Peclet number so that it is significantly elongated along the axial direction where convection dominates over diffusion;
2. the vortical flow surrounding the firewhirl is modelled by a Burgers vortex, whose stream function is a quadratic function of the radial coordinate;
3. the flow has constant density and mass diffusivity;
4. the flow has a unity Lewis number.

By introducing the stream-function coordinates, Chuah *et al*. obtained a Burke-Schumann-like convection-diffusion equation for the mixture fraction, Z, as

$$\frac{\partial Z}{\partial \xi} = \frac{1}{\eta}\frac{\partial}{\partial \eta}\left(\eta \frac{\partial Z}{\partial \eta}\right)$$

where the streamwise (the ξ-direction) convection is balanced by the traverse (the η-direction) diffusion. The flame height of the firewhirl is defined by the farthest axial location satisfying local stoichiometry, $Z = Z_{st}$. The flame height in physical coordinates, x_h, scaled by the diameter of the liquid fuel containing pan d_0, is given by

$$\frac{x_h}{d_0} = \frac{Pe}{16 Z_{st}}$$

which verifies the experimental observation of $x_h/d_0 = O(Pe)$ because $16Z_{st}$ is near unity for common liquid fuels. Although the theory predicts the correct trend of the flame height increasing with Pe, it significantly underestimates the experimental results in the presence of strong vertical flows.

Postulating that the vortical flow surrounding the firewhirl cannot be properly modelled by the Burgers vortex, Klimenko and Williams established a theory by retaining the above approximations 1, 3 and 4 but replacing the approximation 2 with a strong vortex model [18, 23]. The stream function of the strong vortex is a power function of the radial coordinate, and the power exponent α_v is smaller than two. The same Burke-Schumann-like transport equation for the mixture fraction was derived and a modified flame height expression [18] was given by

$$\frac{x_h}{d_0} = \frac{2}{\alpha_v}\frac{Pe}{16Z_{st}}$$

which explains the experimental data because the multiplicative factor, $2/\alpha_v > 1$, accounts for the additional stretching effect of the strong vortex in elongating the firewhirl.

The approximation 3 was adopted by both theoretical studies above, although its physical unreality was already recognized [18]. The temperature variation in the firewhirl flow field causes the corresponding variations of density and mass diffusivity, which may have significant influence on predictions of flame height. Yu and Zhang [19] established a theory with the approximations 1, 2 and 4 but discarded the approximation 3 by taking into account of temperature-dependent density and diffusivities. Unlike the earlier studies based on the mixture-fraction formulation, they adopted the coupling function formulation to obtain temperature solutions. A Howarth-Dorodnitsyn-like density-mass-diffusivity-weighted coordinate transformation was introduced to transform the coupling function formulation into the same Burke-Schumann-like transport equation. A revised flame height expression was accordingly given by

$$\frac{x_h}{d_0} = \left(\frac{T_m}{T_0}\right)^{2-\alpha_T}\frac{Pe}{16Z_{st}}$$

which also explains the experimental data [3]. Here the mean flame temperature, T_m, is higher than

the liquid pool temperature, T_0, the exponent, α_T, characterizing the temperature dependence of mass diffusivity, is always smaller than 2. Consequently, the multiplicative factor, $(T_m/T_0)^{2-\alpha_T} > 1$, accounts for the physics that the temperature rise inside the firewhirl reduces the density and hence the inertia of the fuel vapor, which thereby can be advected to a higher altitude.

It has been recognized that the effects of variable physical properties and the strong vortex model are independent physical mechanisms for explaining the "enhanced" flame height [18, 19]. As a result, integrating these two flame "enhancement" mechanisms in a theory must overshot the predictions of the flame height, and an additional flame "reduction" mechanism must exist to counteract the effects. Based on those considerations, Yu and Zhang [20] recently established a theory, in which the approximations 1 and 4 are retained, temperature-dependent physical properties and a generalized piece-wise power-law vortex model are adopted, and, in addition, the mass diffusivities on the fuel and oxidizer sides of the firewhirl are considered distinctly different (i.e. $D_F \neq D_O$). By use of approximate matching solutions to the species-enthalpy coupling functions with jumping mass diffusivities across the flame sheet, Yu and Zhang [20] derived an integrated expression of the flame height, consisting of four multiplicative factors, as

$$\frac{x_h}{d_0} = \alpha_D \frac{2}{\alpha_{v,\text{eff}}} \left(\frac{T_m}{T_0}\right)^{2-\alpha_T} \frac{Pe}{16 Z_{st}}$$

where the mass-diffusivity-ratio model correction, $\alpha_D = D_F/D_O < 1$, contributes a significant "reduction" mechanism for the flame height and therefore avoid the theoretical overshooting; $\alpha_{v,\text{eff}} < 2$, an analog of α_v in Klimenko and William's theory, is an effective exponent for the piece-wise power-law vortex model.

In summary, of the four major approximations adopted in Chuah *et al.*'s theory, the experimentally verified large Peclet number approximation is indispensable for deriving the analytically solvable Burke-Schumann-like transport equation; the Burgers vortex model and constant physical properties have been examined and revised by Klimenko and Williams[18] and Yu and Zhang[19]; the unity-Lewis number assumption, which can seldom be exactly satisfied in combustion problems [24, 25], has not be examined in all the previous theories. Therefore, the

present study aims to theoretically investigate the effects of non-unity Lewis number on the circulation-controlled firewhirls. Furthermore, the previous study of Yu and Zhang [20] has revealed the "reduction" mechanism for the flame height owing to the mass-diffusivity-ratio model correction, which was however based on the approximate matching solutions. Consequently, the present study also attempts to give a mathematically rigorous treatment to further validate the model correction by addressing unequal Lewis numbers across the flame sheet. In this regard, the present study considers the effects of differential diffusion in general because the Lewis numbers are not only non-unity but also different across the flame sheet.

For a flame-sheet problem with non-unity and unequal Lewis numbers, the conventional coupling-function or mixture-fraction formulations are inapplicable. If the problem is one-dimensional, one can solve the convection-diffusion ODEs (ordinary differential equation) separately on the fuel and oxidizer sides and then match the solutions by using proper jumping conditions at the location of flame sheet, which is simultaneously determined by the matching. Although such a solution procedure has been successfully applied to droplet combustion [26, 27] and other one-dimensional problems [24], it is inapplicable for two- or three-dimensional flame-sheet problems, in which the convection-diffusion PDEs (partial differential equation) cannot be analytically solved with the boundary conditions specified at the undetermined two- or three-dimensional flame sheet.

In the present paper, we shall first mathematically formulate a steady, axisymmetric circulation-controlled firewhirl system with non-unity and unequal Lewis numbers, in Section 2. We then present a perturbation theory to obtain mathematically rigorous solutions to the formulation by assuming the Lewis numbers on the fuel and oxidizer sides are close to unity, in Section 3. The flame shape and the flame height will be derived in explicit forms, and the effects of non-unity and unequal Lewis numbers will be discussed in detail for their physical implications, in Sections 4 and 5. Finally, we shall establish an approximate far-field similarity solution to a mixture-fraction formulation with arbitrary Lewis numbers, thus further verifying and extending the perturbation theory, in Section 6.

Nomenclature

Physical quantities

c_p	constant pressure specific heat
$d_0(r_0)$	diameter (radius) of the fuel liquid pool
D	mass diffusivity
q_c	heat of combustion per unit mass of fuel
q_v	latent heat of vaporization per unit mass of fuel
r, x, ϕ	cylindrical coordinates
T	temperature
u, v, w	velocity components in x, r, ϕ directions
W	molecular weight
Y	mass fraction
Z	mixture fraction
Z_{st}	stoichiometric mixture fraction
α_D	ratio of mass diffusivities, $\alpha_D = D_F/D_O$
α_{v1}	exponent in power-law vortex model (inside vortex core)
α_{v2}	exponent in power-law vortex model (outside vortex core)
α_v	overall exponent in power-law vortex model
α_T	parameter characterizing temperature-dependent mass diffusivity

α_Z coefficient in the transport equation of mixture fraction

λ thermal conductivity

ρ density

σ_{FO} stoichiometric mass ratio $\sigma_{FO} = \nu'_O W_O/(\nu'_F W_F)$

η_c the vortex core radius in $\xi - \eta$ space.

Average quantities at $x = 0$

$Q_0 = \frac{1}{r_0}\int_0^{r_0} Q(0,r)dr\,,\ Q = (T, u, Y_F, \rho, D)$

Non-dimensional and normalized variables

$\tilde{Q} = Q/Q_0\,,\ Q = (D, Y_F, \rho)$

$(\tilde{x}, \tilde{r}) = (x, r)/r_0$

$(\tilde{u}, \tilde{v}) = (u, v)/u_0$

$\tilde{T} = c_p T/q_c$

$\tilde{Y}_O = Y_O/\sigma_{FO}$

Nondimensional number

$Le_F = \lambda/\rho c_p D_F$

$Le_O = \lambda/\rho c_p D_O$

$Pe = u_0 d_0/D_{F0}$

Transformed coordinates

(χ, ζ) stream function coordinates

(ξ, η) density-mass-diffusivity-weighted coordinates

Subscripts

O physical quantities on the oxidizer side of firewhirl

F physical quantities on the fuel side of firewhirl

N physical quantities of inert gas and products

0 physical quantities at $x = 0$

∞ physical quantities in the far field

2. Mathematical Formulation

2.1 Governing Equations

The circulation-controlled firewhirl can be modelled as a steady, non-premixed flame sheet in an axisymmetric, laminar, vortical flow that is free of buoyance effects. Unlike the previous studies assuming unity Lewis number and hence adopting the mathematical formulations of either mixture fraction or conventional coupling function, the present study considers the general situation that the Lewis numbers on the fuel and oxidizer sides of the flame sheet, Le_F and Le_O, are non-unity and unnecessarily equal to each other. By linearly combining the governing equations for the mass fractions of fuel and oxidizer, we can eliminate the chemical reaction terms in the equations and have

$$\left(\rho u \frac{\partial}{\partial x} + \rho v \frac{\partial}{\partial r}\right)\left(Y_F - \frac{Y_O}{\sigma_{FO}}\right) - \frac{\partial}{\partial x}\left(\rho D_F \frac{\partial Y_F}{\partial x} - \frac{1}{\sigma_{FO}} \rho D_O \frac{\partial Y_O}{\partial x}\right) - \frac{1}{r}\frac{\partial}{\partial r}\left(\rho D_F r \frac{\partial Y_F}{\partial r} - \frac{1}{\sigma_{FO}} \rho D_O r \frac{\partial Y_O}{\partial r}\right) = 0 \tag{1}$$

Similarly, linearly combining the governing equations for the mass fraction of fuel and the sensible

enthalpy to eliminate the chemical reaction terms yields

$$\left(\rho u\frac{\partial}{\partial x}+\rho v\frac{\partial}{\partial r}\right)\left(Y_F+\frac{c_pT}{q_c}\right)-\frac{\partial}{\partial x}\left(\rho D_F\frac{\partial Y_F}{\partial x}+\frac{\lambda}{q_c}\frac{\partial T}{\partial x}\right)$$
$$-\frac{1}{r}\frac{\partial}{\partial r}\left(\rho D_F r\frac{\partial Y_F}{\partial r}+\frac{\lambda}{q_c}r\frac{\partial T}{\partial r}\right)=0 \quad (2)$$

It is readily seen that, for the special situation of $Le_F = Le_O = 1$ and $D_F = D_O$, Equations (1) and (2) can be simplified to the transport equations of the conventional species-species coupling function, defined by $Y_F - Y_O/\sigma_{FO}$, and of the species-enthalpy coupling function, defined by $Y_F + c_pT/q_c$, respectively.

The boundary conditions for Equations (1) and (2) are specified as follows: the axisymmetric boundary condition at the axis is written by

BC(1) at $r = 0,\ \partial Y_F/\partial r = \partial Y_O/\partial r = \partial T/\partial r = 0.$

The natural boundary condition in the far-field radial direction is given by

BC(2) at $r \to \infty,\ \partial Y_F/\partial r = \partial Y_O/\partial r = \partial T/\partial r = 0.$

The ground boundary at $x = 0$ can be divided into the fuel side $(r < r_0)$ and the oxidizer side $(r > r_0)$ because the flame-sheet is anchored at the circular rim of the fuel pool $(r = r_0)$. The corresponding boundary conditions are given by

BC(3a) at $x = 0$ and $r < r_0,\ Y_F = Y_{F0},\ Y_O = 0,\ T = T_0,$

BC(3b) at $x = 0$ and $r > r_0,\ \partial Y_F/\partial x = \partial Y_O/\partial x = \partial T/\partial x = 0.$

The flame-sheet approximation, implying an infinitely fast reaction rate, renders no fuel leakage across the flame and yields another far-field boundary condition as

BC(4) at $x \to \infty,\ Y_F = 0,\ Y_O = Y_{O\infty}$, and $T = T_\infty$.

It is noted that BCs (3a) contains two unspecified quantities, Y_{F0} and T_0, whose determination is a part of the "closure problem" that has been discussed in detail in the previous papers[19, 20]. For

a complete and clear presentation of the present theory, we summarized and further clarified the closure problem in Appendix A.

It is also noted that a divergent flux at the burner rim (i.e., the periphery of the liquid pool, $r = r_0$) exists in all the flame-sheet theories of firewhirls. Chuah *et al*. [8, 11] pointed out that the flame is actually quenched at the burner rim due to the heat loss so that a small quenching distance separates the flame from the burner. They also pointed out that, although the flame-sheet theory cannot be applied to the location of $r = r_0$, the predicted firewhirl characteristics is not affected. This singularity problem could be remedied by establishing a revised theory with finite reaction rate, therefore allowing local flame extinction. Such a theory, focusing on the anchoring region of the diffusion flame [28], certainly merits future studies but will not considered in the present study.

2.2 Large-Peclet-number Formulation

A crucial procedure in formulating the present problem considering variable physical properties is to introduce the density-mass-diffusivity-weighted coordinate defined by

$$\xi = \frac{D_{F0}}{u_0 r_0}\int_0^{\tilde{x}} \tilde{\rho}^2 \tilde{D}_F dx' = \frac{2}{Pe}\int_0^{\tilde{x}} \tilde{\rho}^2 \tilde{D}_F dx', \qquad \eta = \int_0^{\tilde{r}} \tilde{\rho} dr' \tag{3}$$

This is an analog of the well-known Howarth-Dorodnitsyn transformation, which was widely used in compressible boundary layer problems [29]. The procedure has been adopted and validated by the previous studies [19, 20].

Applying the coordinate transformation (3) and the large Peclet number approximation, $Pe \gg 1$, to Equations (1) and (2), we have the following non-dimensional parabolic PDEs in the (ξ, η) coordinate system:

$$\left(\hat{u}\frac{\partial}{\partial \xi} + \hat{v}\frac{\partial}{\partial \eta}\right)\left(\tilde{Y}_F + \tilde{T}\right) = Le_F \frac{1}{\eta}\frac{\partial}{\partial \eta}\left[\eta \frac{\partial}{\partial \eta}\left(\frac{\tilde{Y}_F}{Le_F} + \tilde{T}\right)\right] \tag{4}$$

$$\left(\hat{u}\frac{\partial}{\partial\xi}+\hat{v}\frac{\partial}{\partial\eta}\right)\left(\tilde{Y}_F-\tilde{Y}_O\right)=Le_F\frac{1}{\eta}\frac{\partial}{\partial\eta}\left[\eta\frac{\partial}{\partial\eta}\left(\frac{\tilde{Y}_F}{Le_F}-\frac{\tilde{Y}_O}{Le_O}\right)\right] \tag{5}$$

It is noted that, regardless of the coordinate "shrinking" due to the variations of density and mass diffusivity, the axial coordinate, x, is scaled by a factor of $2/Pe$ to account for that the firewhirl with $Pe \gg 1$ is significantly stretched along the axial direction. As a result, the convection terms and the radial diffusion term are of $O(1)$ in Equations (4) and (5); the axial diffusion term is of $O(Pe^{-1})$ and therefore can be neglected.

The corresponding non-dimensional boundary conditions are given by

BC(I) at $\eta = 0,\ \partial\tilde{Y}_F/\partial\eta = \partial\tilde{Y}_O/\partial\eta = \partial\tilde{T}/\partial\eta = 0$

BC(II) at $\eta \to \infty,\ \partial\tilde{Y}_F/\partial\eta = \partial\tilde{Y}_O/\partial\eta = \partial\tilde{T}/\partial\eta = 0$

BC(III-a) at $\xi = 0$ and $\eta \le 1,\ \tilde{Y}_F = \tilde{Y}_{F0},\ \tilde{T} = \tilde{T}_0,\ \tilde{Y}_O = 0$

BC(III-b) at $\xi = 0$ and $\eta > 1,\ \tilde{Y}_F = 0,\ \tilde{T} = \tilde{T}_\infty,\ \tilde{Y}_O = \tilde{Y}_{O\infty}$

It is noted that BC(4) is not compatible with the parabolic PDE system and therefore can be removed from the present large-Peclet-number formulation. The complex derivations for the above equations and boundary conditions are similar to those given in the previous paper [20] except that two distinct Lewis numbers remain in the present equations. The details of the derivations are expatiated in Appendix B.

A few remarks should be given to the boundary conditions BC(III-b). Replacing the Neumann boundary condition BC(3b) by the Dirichlet boundary condition BC(III-b) implies that the ground surface outside the fuel pool is assumed to be isothermal. Although this isothermal assumption is not required by the mixture fraction formulations [3, 18], it brings significant mathematical convenience to the coupling-function formulations to derive the Burke-Schumann-like transport equation. At the cost of mathematical complexities, we can formulate a theory with a ground temperature profile $\tilde{T}_w$, which however cannot be specified without experimental data. As discussed in the previous study [20], the scaled wall temperature $\tilde{T}_w$ is significantly smaller than the flame temperature $\tilde{T}_f$

therefore considering the difference between $\tilde{T}_w$ and $\tilde{T}_\infty$ is unlikely to have significant influence on flame shape of the firewhirl.

2.3 Burke-Schumann-like Transport Equation in Stream-function Coordinates

For a convection-diffusion system like Equations (4) and (5), a stream-function coordinate can be introduced to the eliminate the streamwise convection term (i.e. the $\partial/\partial\xi$ term) [3, 18-20, 23], as long as the stream function is a power-law function of the traverse coordinate (i.e. the η coordinate), $\psi \sim \eta^{\alpha_v}$, where α_v is the power exponent. Consequently, we introduced the stream-function coordinates, (χ, ζ), defined by

$$\chi = \frac{\alpha_v}{2}\xi, \qquad \zeta = \sqrt{2\psi} \tag{6}$$

and Equations (4) and (5) can be rewritten by

$$\frac{\partial}{\partial\chi}\left(\tilde{Y}_F + \tilde{T}\right) = Le_F \frac{1}{\zeta}\frac{\partial}{\partial\zeta}\left[\zeta\frac{\partial}{\partial\zeta}\left(\frac{\tilde{Y}_F}{Le_F} + \tilde{T}\right)\right] \tag{7}$$

$$\frac{\partial}{\partial\chi}\left(\tilde{Y}_F - \tilde{Y}_O\right) = Le_F \frac{1}{\zeta}\frac{\partial}{\partial\zeta}\left[\zeta\frac{\partial}{\partial\zeta}\left(\frac{\tilde{Y}_F}{Le_F} - \frac{\tilde{Y}_O}{Le_O}\right)\right] \tag{8}$$

Accordingly, the boundary conditions in the stream-function coordinates are given by

BC(i) at $\zeta = 0$, $\partial\tilde{Y}_F/\partial\zeta = \partial\tilde{Y}_O/\partial\zeta = \partial\tilde{T}/\partial\zeta = 0$,

BC(ii) at $\zeta \to \infty$, $\partial\tilde{Y}_F/\partial\zeta = \partial\tilde{Y}_O/\partial\zeta = \partial\tilde{T}/\partial\zeta = 0$,

BC(iii-a) at $\chi = 0$ and $\zeta \le 1$, $\tilde{Y}_F = \tilde{Y}_{F0}$, $\tilde{T} = \tilde{T}_0$, $\tilde{Y}_O = 0$,

BC(iii-b) at $\chi = 0$ and $\zeta > 1$, $\tilde{Y}_F = 0$, $\tilde{T} = \tilde{T}_\infty$, $\tilde{Y}_O = \tilde{Y}_{O\infty}$.

Equations (7) and (8) subject to BC(i)-BC(iii) constitute the analytically solvable Burke-Schumann-like formulation to be solved in the following sections.

3. Perturbation theory for near-unity Lewis numbers

3.1 Perturbation Formulation

As we have discussed in Introduction, analytically solving Equations (7) and (8) with arbitrary Le_F and Le_O are mathematically impossible. Nevertheless, the equations for the particular case of $Le_F \approx 1$ and $Le_O \approx 1$ can be analytically solved in the framework of perturbation theory by regarding the deviations of the Lewis numbers from unity as small parameters.

We introduced the Lewis-number-weighted coupling functions as

$$\beta_S = \frac{\tilde{Y}_F}{Le_F} - \frac{\tilde{Y}_O}{Le_O}, \qquad \beta_T = \frac{\tilde{Y}_F}{Le_F} + \tilde{T} \tag{9}$$

which are continuous and smooth at the flame location [30] in contrast to the continuous but non-smooth conventional coupling functions. This can readily be seen from the jump condition $\left[\partial\left(\tilde{Y}_F/Le_F\right)/\partial n\right]^+ = \left[\partial\left(\tilde{Y}_O/Le_O\right)/\partial n\right]^-$, where $\partial/\partial n$ represents the directional derivative normal to the local flame surface, and the superscripts "+" and "−" indicate the derivatives being evaluated in the fuel and oxidizer sides of the flame. It is noted that the Lewis-number-weighted coupling functions are similar to the generalized mixture fractions defined by Liñán *et al*. [28].

In terms of the Lewis-number-weighted coupling functions, Equations (7) and (8) can be rewritten by

$$\frac{\partial \beta_T}{\partial \chi} - Le_F \frac{1}{\zeta}\frac{\partial}{\partial \zeta}\left(\zeta \frac{\partial \beta_T}{\partial \zeta}\right) = -\left(1 - \frac{1}{Le_F}\right)\frac{\partial \tilde{Y}_F}{\partial \chi} \tag{10}$$

$$\frac{\partial \beta_S}{\partial \chi} - Le_F \frac{1}{\zeta}\frac{\partial}{\partial \zeta}\left(\zeta \frac{\partial \beta_S}{\partial \zeta}\right) = -\left(1 - \frac{1}{Le_F}\right)\frac{\partial \tilde{Y}_F}{\partial \chi} + \left(1 - \frac{1}{Le_O}\right)\frac{\partial \tilde{Y}_O}{\partial \chi} \tag{11}$$

Without losing generality, we assume that Le_F is not equal to but close to unity and introduce a small parameter

$$\epsilon = 1 - \frac{1}{Le_F} \tag{12}$$

and hence have

$$1-\frac{1}{Le_O}=\frac{Le_F}{Le_O}\frac{Le_O-1}{Le_F-1}\epsilon=c_O\epsilon \tag{13}$$

Here $|\epsilon|\ll 1$ and $c_O=O(1)$. Consequently, the coupling functions can be expanded in the asymptotic series in terms of ϵ up to the first order term as

$$\beta_S=\beta_S^{(0)}+\epsilon\beta_S^{(1)}+O(\epsilon^2) \tag{14}$$

$$\beta_T=\beta_T^{(0)}+\epsilon\beta_T^{(1)}+O(\epsilon^2) \tag{15}$$

Substituting Equations (12)-(15) into Equations (10) and (11) and collecting the terms of the same orders, we have the parabolic, inhomogeneous PDEs for the leading-order denoted by the superscript ($i=0$) and the first-order ($i=1$) coupling functions as

$$\hat{L}_{\chi,\zeta}\beta_T^{(i)}=h_T^{(i)},\qquad \hat{L}_{\chi,\zeta}\beta_S^{(i)}=h_S^{(i)} \tag{16}$$

where $\hat{L}_{\chi,\zeta}$ is a Burke-Schumann-like partial differential operator in the (χ,ζ) coordinates

$$\hat{L}_{\chi,\zeta}=\frac{\partial}{\partial\chi}-Le_F\frac{1}{\zeta}\frac{\partial}{\partial\zeta}\left(\zeta\frac{\partial}{\partial\zeta}\right) \tag{17}$$

and $h_T^{(i)}$ and $h_S^{(i)}$ are the source terms given by

$$h_T^{(i)}=\begin{cases}0, & i=0\\ -\dfrac{\partial\tilde{Y}_F^{(0)}}{\partial\chi}, & i=1\end{cases} \tag{18}$$

$$h_S^{(i)}=\begin{cases}0, & i=0\\ -\dfrac{\partial\tilde{Y}_F^{(0)}}{\partial\chi}+c_O\dfrac{\partial\tilde{Y}_O^{(0)}}{\partial\chi}, & i=1\end{cases} \tag{19}$$

The leading-order fuel and oxidizer mass fractions, $\tilde{Y}_F^{(0)}$ and $\tilde{Y}_O^{(0)}$, can be obtained by the linear combinations of the leading-order coupling functions $\beta_S^{(0)}$ and $\beta_T^{(0)}$. Specifically, $\tilde{Y}_F^{(0)}=Le_F\beta_S^{(0)}$

on the fuel side of the flame, and $\tilde{Y}_O^{(0)} = -Le_O \beta_S^{(0)}$ on the oxidizer side.

Correspondingly, the leading-order and the first-order boundary conditions can be rewritten by

BC(1) at $\zeta = 0,\ \partial\beta_S^{(i)}/\partial\zeta = \partial\beta_T^{(i)}/\partial\zeta = 0,$

BC(2) at $\zeta \to \infty,\ \partial\beta_S^{(i)}/\partial\zeta = \partial\beta_T^{(i)}/\partial\zeta = 0,$

BC(3-a) at $\chi = 0$ and $\zeta \le 1,\ \beta_S^{(i)} = b_{Sa}^{(i)},\ \beta_T^{(i)} = b_{Ta}^{(i)},$

BC(3-b) at $\chi = 0$ and $\zeta > 1,\ \beta_S^{(i)} = b_{Sb}^{(i)},\ \beta_T^{(i)} = b_{Tb}^{(i)}.$

where the Dirichlet boundary conditions are given by

$$b_{Sa}^{(i)} = \begin{cases} \tilde{Y}_{F0}/Le_F, & i = 0 \\ 0, & i = 1 \end{cases}, \quad b_{Ta}^{(i)} = \begin{cases} \tilde{Y}_{F0}/Le_F + \tilde{T}_0, & i = 0 \\ 0, & i = 1 \end{cases} \tag{20}$$

$$b_{Sb}^{(i)} = \begin{cases} -\tilde{Y}_{O\infty}/Le_O, & i = 0 \\ 0, & i = 1 \end{cases}, \quad b_{Tb}^{(i)} = \begin{cases} \tilde{T}_\infty, & i = 0 \\ 0, & i = 1 \end{cases} \tag{21}$$

3.2 Perturbation Solutions

The leading-order coupling functions, $\beta_S^{(0)}$ and $\beta_T^{(0)}$, satisfy the homogeneous transport equations with inhomogeneous Dirichlet boundary conditions at $\chi = 0$. These leading-order equations and boundary conditions are of identical forms to those that have been solved in the previous studies [19, 20] for unity Lewis number. Consequently, we can directly write the solutions as

$$\beta_S^{(0)} = -\frac{\tilde{Y}_{O,\infty}}{Le_O} + \left(\frac{\tilde{Y}_{F,0}}{Le_F} + \frac{\tilde{Y}_{O,\infty}}{Le_O}\right)\int_0^\infty J_0(\omega\zeta)J_1(\omega)\exp(-Le_F\omega^2\chi)d\omega \tag{22}$$

$$\beta_T^{(0)} = \tilde{T}_\infty + \left(\frac{\tilde{Y}_{F,0}}{Le_F} + \tilde{T}_0 - \tilde{T}_\infty\right)\int_0^\infty J_0(\omega\zeta)J_1(\omega)\exp(-Le_F\omega^2\chi)d\omega \tag{23}$$

where J_n denotes the Bessel function of the first kind of order n.

The first-order coupling functions, $\beta_S^{(1)}$ and $\beta_T^{(1)}$, satisfy inhomogeneous transport equations with homogeneous boundary conditions on all sides. The source terms in the first-order equations can be determined by using the leading-order solutions (22) and (23). Therefore, the first-order solutions can be obtained by means of Green's function method.

The Green's function for the partial differential operator (17), denoted by $G(\chi, \chi', \zeta, \zeta')$, is defined by

$$\hat{L}_{\chi,\zeta} G(\chi, \chi', \zeta, \zeta') = \delta(\chi - \chi')\delta(\zeta - \zeta') \tag{24}$$

where $\delta(\chi - \chi')$ and $\delta(\zeta - \zeta')$ are Dirac's delta functions, and therefore satisfies the normalization relation,

$$\int_{\mathcal{D}} \hat{L}_{\chi,\zeta} G(\chi, \chi', \zeta, \zeta') d\mathcal{V} = 1 \tag{25}$$

where $d\mathcal{V} = \zeta d\zeta d\chi$ is the differential element of the domain $\mathcal{D}(\chi, \xi) = [(0, \infty) \times (\infty, -\infty)]$. Equation (25) indicates that $G(\chi, \chi', \zeta, \zeta')$ can be regarded as the inverse operator of $\hat{L}_{\chi,\zeta}$, namely $G = \hat{L}_{\chi,\zeta}^{-1}$, so that the LHS of Equation (25) can be treated as an inner product of two operators in the Hilbert space [31]. As a result, the first-order solutions to Equation (10) and (11) can be formally given by

$$\beta_S^{(1)} = \hat{L}_{\chi,\zeta}^{-1} h_S^{(1)}, \qquad \beta_T^{(1)} = \hat{L}_{\chi,\zeta}^{-1} h_T^{(1)} \tag{26}$$

Substituting Equations (18) and (19) into Equation (26) and again regarding its RHS as the inner product of two operators, we have

$$\beta_T^1(\chi, \zeta) = -\int_0^\infty d\chi' \int_0^\infty G(\chi, \chi', \zeta, \zeta') \frac{\partial \tilde{Y}_F^{(0)}}{\partial \chi'} \zeta' d\zeta' \tag{27}$$

$$\beta_S^1(\chi,\zeta) = -\int_0^\infty d\chi' \int_0^\infty G(\chi,\chi',\zeta,\zeta')\left(\frac{\partial \tilde{Y}_F^{(0)}}{\partial \chi'} - c_O \frac{\partial \tilde{Y}_O^{(0)}}{\partial \chi'}\right)\zeta' d\zeta' \tag{28}$$

The Green's function $G(\chi,\chi',\zeta,\zeta')$ can be constructed by means of eigenfunction expansion [31], and is given by

$$G(\chi,\chi',\zeta,\zeta') = H(\chi-\chi')\int_0^\infty \omega J_0(\omega\zeta')J_0(\omega\zeta)\exp[-\omega^2 Le_F(\chi-\chi')]d\omega \tag{29}$$

where $H(\chi-\chi')$ is Heaviside step function. The mathematically complex procedure for deriving Equation (29) will not be presented in the paper, but the validity of Equation (29) can be readily verified, as shown in Appendix C.

3.3 Series Solutions of $\boldsymbol{\beta_S}$ and $\boldsymbol{\beta_T}$

To simplify the first-order couple functions, $\beta_S^{(1)}$ and $\beta_T^{(1)}$, from Equations (27) and (28), we should first evaluate the derivatives of the leading-order mass fractions, $\tilde{Y}_F^{(0)}$ and $\tilde{Y}_O^{(0)}$, with respect to χ'. According to the definition of the leading-order coupling functions, $\tilde{Y}_F^{(0)} = Le_F\beta_S^{(0)}$ on the fuel side of the flame sheet and $\tilde{Y}_O^{(0)} = -Le_O\beta_S^{(0)}$ on the oxidizer side. Consequently, we have

$$\frac{\partial}{\partial \chi'}\tilde{Y}_F^{(0)}(\chi',\zeta') = -Le_F^2\left(\frac{\tilde{Y}_{F0}}{Le_F} + \frac{\tilde{Y}_{O\infty}}{Le_O}\right)J(\chi',\zeta') \tag{30}$$

and

$$\frac{\partial}{\partial \chi'}\tilde{Y}_O^{(0)}(\chi',\zeta') = Le_F Le_O\left(\frac{\tilde{Y}_{F0}}{Le_F} + \frac{\tilde{Y}_{O\infty}}{Le_O}\right)J(\chi',\zeta') \tag{31}$$

where $J(\chi',\zeta')$ is an integral function defined by

$$J(\chi',\zeta') = \int_0^\infty \varpi^2 J_0(\varpi\zeta')J_1(\varpi)\exp(-Le_F\varpi^2\chi')d\varpi \tag{32}$$

Substituting the Green's function (29) and the derivatives (30) and (31) into Equations (27) and (28), and noting that $\tilde{Y}_F^{(0)}$ and $\tilde{Y}_O^{(0)}$ vanish on the oxidizer and fuel sides, respectively, we have

$$\beta_S^{(1)} = Le_F^2\left(\frac{\tilde{Y}_{F0}}{Le_F}+\frac{\tilde{Y}_{O\infty}}{Le_O}\right)\left[I_F+\frac{Le_O}{Le_F}c_O I_O\right] \tag{33}$$

$$\beta_T^{(1)} = Le_F^2\left(\frac{\tilde{Y}_{F0}}{Le_F}+\frac{\tilde{Y}_{O\infty}}{Le_O}\right)I_F \tag{34}$$

where I_F and I_O represents four-fold integrals defined on the fuel and oxidizer domains, respectively, as

$$I_F(\chi,\zeta) = \int_0^{\chi_f}\int_0^{\zeta_f} G(\chi,\chi',\zeta,\zeta')J(\chi',\zeta')\zeta' d\zeta' d\chi' \tag{35}$$

$$I_O(\chi,\zeta) = \left[\int_0^{\chi_f}\int_{\zeta_f}^{\infty}+\int_{\chi_f}^{\infty}\int_0^{\infty}\right] G(\chi,\chi',\zeta,\zeta')J(\chi',\zeta')\zeta' d\zeta' d\chi' \tag{36}$$

whose simplified forms will be given in the following sections.

It is noted that the above solution of β_S cannot be directly applied to the degenerate situation of $Le_F = 1$, which results a singular c_O. Although $Le_F = 1$ is reasonably accurate only for methane and $Le_O = 1$ is often found an acceptable approximation [28], we also considered the degenerate situation of $Le_F = 1$ while $Le_O \neq 1$ to complement our theory. Consequently, we can expand β_S by regarding the deviation of Le_O from unity as small parameter, denoted by $\epsilon' = 1 - 1/Le_O$, and have

$$\beta_S = \beta_S^{(0)} + \epsilon'\beta_S^{(1)\prime} \tag{37}$$

in which the modified first order solution can be written as

$$\beta_S^{(1)\prime} = Le_F Le_O\left(\frac{\tilde{Y}_{F0}}{Le_F}+\frac{\tilde{Y}_{O\infty}}{Le_O}\right)I_O \tag{38}$$

By comparing Equation (38) with Equation (33), we can see that Equation (38) can be formally obtained from Equation (33) by replacing $c_O\epsilon$ by ϵ' and by setting all the other terms containing ϵ to be zero. This procedure can be applied in the following sections for obtaining the results concerning with the degenerate situation of $Le_F = 1$ and $Le_O \neq 1$.

4. Flame Characteristics of Firewhirls

4.1 Approximate Solutions of Flame Shape

In most previous studies, the flame height of firewhirls was the central focus of research, whereas the flame shape was barely investigated. It is of interest in the present study to derive approximate analytical solutions of flame shape for illustrating the flame characteristics of firewhirls.

In the flame-sheet theory, both fuel and oxidizer are completely consumed according to stoichiometry, rendering $\beta_S = \beta_S^{(0)} + \epsilon\beta_S^{(1)} = 0$ on the flame sheet. Consequently, with Equation (22) for $\beta_S^{(0)}$ and Equation (33) for $\beta_S^{(1)}$, the flame shape can be determined in an implicit form as

$$\frac{Z_{st}}{Le_O} = (1-\epsilon)\int_0^\infty J_0(\omega\zeta_f)J_1(\omega)\exp(-Le_F\omega^2\chi_f)d\omega + \epsilon Le_F^2\left[I_F(\chi_f,\zeta_f) + \frac{Le_O}{Le_F}c_O I_O(\chi_f,\zeta_f)\right] \tag{39}$$

where the stoichiometric mixture fraction defined by $Z_{st} = \tilde{Y}_{O\infty}/(\tilde{Y}_{F0} + \tilde{Y}_{O\infty})$ is introduced for direct comparison with the previous studies. It is noted that we have ignore the higher-order small terms containing $Z_{st}\epsilon$ because of $Z_{st} \ll 1$ for most common liquid fuels. Several further simplifications can be made to the flame shape expression as follows.

For the flame close to the fuel pool, namely $\chi_f = O(\epsilon)$, the four-fold integrals I_F and I_O tend to be of order $O(\epsilon)$, as proved in Appendix D, and hence the second term on the RHS of Equation (39) is of $O(\epsilon^2)$ and can be neglected. Mathematically, this means that the flame shape close to the fuel pool is determined by leading-order solution of the coupling function. Physically, the flame is anchored around the rim of the fuel pool and thus its local shape is modulated by the dimension of

the fuel pool rather than physicochemical properties of the flame.

For the flame being away from the fuel pool, namely $\chi_f = O(1)$, the integral I_F is proportional to $\zeta_f^2/16$, as proved in (D5) of Appendix D, and can be neglected. Here we have used the result that $\zeta_f \ll 1$ at the flame location $\chi_f = O(1)$ because the flame sheet is close to the axis in the far field [20]. Therefore, the first-order correction owing to I_O should be considered in determining the flame shape, particularly in determining the flame height to be discussed in the following subsection. As a result, Equation (39) can be simplified as

$$\frac{Z_{st}}{Le_O} = (1-\epsilon)\int_0^\infty J_0(\omega\zeta_f)J_1(\omega)\exp(-Le_F\omega^2\chi_f)d\omega + c_O\epsilon Le_F Le_O\chi_f\int_0^\infty \omega^2 J_0(\omega\zeta_f)J_1(\omega)\exp(-Le_F\omega^2\chi_f)d\omega \tag{40}$$

Furthermore, we noted that the integrals for $\chi_f = O(1)$ are mainly determined by the values of ω close to zero according to the principle of Laplace integration [32]. Consequently, we can analytically integrate Equation (40) by using the approximation, $J_1(\omega) \sim \omega/2$, namely the first term of the Taylor expansion of $J_1(\omega)$ around $\omega = 0$, and have

$$\frac{Z_{st}}{Le_O} = \frac{1}{4Le_F\chi_f}\left(1-\epsilon+c_O\epsilon Le_O\frac{-\zeta_f^2+4Le_F\chi_f}{4Le_F\chi_f}\right)\exp\left(-\frac{\zeta_f^2}{4Le_F\chi_f}\right) \tag{41}$$

which expresses the flame shape in an implicit form for the following discussion.

To derive explicit expressions of the flame shape, we can first neglect all the $O(\epsilon)$ terms in Equation (41) to obtain a leading-order expression as

$$\chi_f' \ln\chi_f' = -\frac{Z_{st}}{Le_O}\zeta_f^2, \tag{42}$$

where χ_f' denotes

$$\chi_f' = 4Z_{st}\frac{Le_F}{Le_O}\chi_f \tag{43}$$

It is interestingly seen that Equation (42) resembles the well-known "$f^2\ln f^2 = -L_v$" [24, 25]

formulas for explaining the premixed flame extinction due to heat loss. This implies that a similar turning point (a turning point on the $f - L_v$ curve corresponding to $L_v = 1/e$) exists on the $\chi_f' - \zeta_f$ curve (i.e. the flame shape) if the RHS of Equation (42) is equal to $-1/e$, yielding $\zeta_f = (Le_O/Z_{st}e)^{1/2} > 1$ because of $Z_{st} \ll 1$ for common liquid fuels. Physically, this turning point, if emerged, is close to the liquid pool, where is however beyond the validity range of the above expression. Consequently, the turning point does not emerge in the real flame shape.

Substituting Equation (42) into the first-order term in Equation (41), we can have the explicit expression as

$$\chi_f' \ln \chi_f' - \chi_f' \ln [1 - \epsilon + c_o \epsilon Le_O \ln(e\chi_f')] = -\frac{Z_{st}}{Le_O}\zeta_f^2 \tag{44}$$

based on which we shall discuss about the influence of non-unity Lewis numbers on the flame shape.

Applying the inverse transformations of Equations (3) and (6) to Equations (41) and (44), which can be regarded as the re-scaling of the radial and axial coordinates according to the vortical flow characteristics and the variations of density and mass diffusivity, we can have the flame shape in physical coordinates.

The flame shapes at different Lewis numbers are plotted in Figure 1, where the transformed coordinate χ is also shown to manifest the influence of the density-mass-diffusivity-weighted coordinate transformation on the axial coordinate at large Peclet number. It is seen that the approximate, explicit solution of the flame shape, namely Equation (44), agrees well with the exact, implicit solution of the flame shape, namely Equation (39), at $x_f > 5$ (or $\chi_f > 0.5$) where the flame is sufficiently away from the fuel pool. This good agreement substantiates the above procedure for approximate solutions.

The deviation of the approximate solution from the exact solution noticeably emerges as the flame is close to the fuel pool, as indicated by the physically unrealistic turning. The mathematical reason is that, at small axial flame locations, the integrals in equation (40) cannot be evaluated asymptotically by using the Laplace integration method based on $\chi_f = O(1)$. As a result, the

approximate solutions cannot be extended to the region within $\chi_f < 0.5$ corresponding to the physical region of $x_f < 5$.

As seen in Figure 1, compared with the case with $Le_F = Le_O = 1$, decreasing the fuel Lewis number to $Le_F = 0.9$ while retaining $Le_O = 1$ substantially stretches the flame shape, particularly in the axial direction. This can be explained by that the smaller Le_F means larger fuel mass diffusivity, which helps transport the fuel vapor to higher altitude and hence results in an elongated flame. On the contrary, decreasing the oxidizer Lewis number to $Le_O = 0.9$ while retaining $Le_F = 1$ substantially compresses the flame shape. This is because the smaller Le_O means larger oxidizer mass diffusivity, which helps transport the oxidizer to lower altitude and hence results in a stout flame. These effects of the fuel and oxidizer Lewis numbers on the flame height are similar to those on the flame stand-off distance in droplet combustion [24, 26, 27]

It is noted that Equation (43) implies that the flame shape largely depends on the Lewis numbers ratio, Le_O/Le_F, rather than on Le_O and Le_F separately. This can be seen from Figure 2 that the calculated flame shapes corresponding to various Le_O and Le_F but a fixed ratio of $Le_O/Le_F = 1$ are only slightly different from each other. In addition, the flame shape with larger Lewis numbers tend to be slimmer than that with lower Lewis numbers. The physical reason can be interpreted as follows. The larger Lewis numbers for both fuel and oxidizer mean lower mass diffusivities so that the axial convection tends to dominate over diffusion, resulting in a more stretched flame shape in the axial direction. For the same reason, lower Lewis numbers for fuel and oxidizer mean enhanced mass diffusion in all the directions, which tends to counteract the axial convection and to make flame shape stouter.

4.2 Flame Height

Understanding the controlling mechanisms of firewhirl flame height is always of importance because the behaviors of firewhirl are usually associated with the change of flame height [2, 4, 11, 12]. With the derived expressions for the flame shape, the determination of the flame height is straightforward by setting $\zeta_f = 0$ in Equation (44), yielding

$$\chi_f = \frac{Le_O}{Le_F}\frac{1}{4Z_{st}}(1-\epsilon+c_o\epsilon Le_O) \tag{45}$$

where all the higher order terms than $O(\epsilon)$ have been neglected. Again, Equation (45) indicates the dependence of the flame height on the Lewis number ratio.

The leading-order flame height is given by setting $\zeta_f = 0$ in Equation (42) or by neglecting all the $O(\epsilon)$ terms in Equation (45),

$$\chi_h^{(0)} = \frac{Le_O}{Le_F}\frac{1}{4Z_{st}} = \frac{D_F}{D_O}\frac{1}{4Z_{st}} = \frac{\alpha_D}{4Z_{st}} \tag{46}$$

which reproduces Yu and Zhang's result on the mass-diffusivity-ratio correction [20] and proves that the effect of distinct mass diffusivities is essentially the leading-order approximation of non-unity Lewis number effect. It should be noted that Equation (46) was derived in [20] based on an approximate matching solution while in the present study based on the mathematically rigorous perturbation theory.

Applying the inverse transformations of Equations (3) and (6) to Equation (45), we have the explicit expression of flame height in physical coordinates as

$$\frac{x_h}{d_0} = \frac{Le_O}{Le_F}\frac{2}{\alpha_v}\left(\frac{T_m^{(0)}}{T_0}\right)^{2-\alpha_T}\frac{Pe}{16Z_{st}}\left(1-\epsilon+c_o\epsilon Le_O+\epsilon\frac{T_m^{(1)}}{T_0}\right) \tag{47}$$

where $T_m^{(0)}$ is the leading-order "average" temperature that has been given in [19, 20] and $T_m^{(1)}$ accounts for the influence of the first-order temperature solution:

$$T_m^{(0)} = \left(\frac{1}{x_h}\int_0^{x_h} {T^{(0)}}^{\alpha_T-2}dx\right)^{1/(\alpha_T-2)}, \qquad T_m^{(1)} = T_0\frac{\int_0^{x_h}{T^{(0)}}^{\alpha_T-3}T^{(1)}dx}{\int_0^{x_h}{T^{(0)}}^{\alpha_T-2}dx} \tag{48}$$

The last term of Equation (47) reflects the fact that the non-unity Lewis numbers also affect the flame temperature [24, 25, 28], which in turn alters the flame height by a factor of order $O(\epsilon)$.

The exponent α_T characterizes the temperature-dependence of mass diffusivities through

$$D_F = D_{F0}\left(\frac{T}{T_0}\right)^{\alpha_T} \tag{49}$$

in which α_T is usually less than 2 and equal to 3/2 in the kinetic theory of gases employing the rigid-sphere model. Consequently, the term $(T_m/T_0)^{2-\alpha_T} > 1$ accounts for the flame height enhancement owing to the effects of variable density and mass diffusivity, which have been thoroughly discussed by Yu and Zhang [20].

The factor $2/\alpha_v$ characterizes the influence of the generalized power-law vortical flow[18, 23, 33] on the flame height, and it is unity for the Burgers vortex model with $\alpha_v = 2$. In the strong vortex model, the exponent should be replaced by its effective value, α_v, being smaller than 2 [18, 23, 33]. Consequently, compared with the Burgers vortex, the strong vortex results in a more rapid axial flow, which tends to elongate the flame height. It is noted that α_v can be determined by considering the compensating regime [18, 23] or by considering a piece-wise power-law vortex model with physical meaningful exponents for inner and outer vortices. The derivation of α_v, which requires the far-field solution of the firewhirl to be expatiated in the following section, has been given by Klimenko and William [18] and Yu and Zhang [20], and therefore will be summarized in Appendix E.

5. Far-field Similarity Solution of Mixture Fraction

Although the above perturbation theory produces the important results about the influence of non-unity and unequal Lewis numbers on the flame characters of the firewhirls, it is rather interesting to verify these results for arbitrary Lewis numbers. As we have discussed in Introduction, the mathematically rigorous treatment to the formulation (7)-(8) is difficult because general solutions to the PDE system on either the fuel side or the oxidizer side are impossible. Consequently, the matching solution approach, which has been used to the ODE systems formulated from one-dimensional combustion problems, is inapplicable here. We can however establish a similarity solution to the formulation with arbitrary Lewis numbers. This solution does not satisfy the boundary condition on the fuel pool and therefore is valid only in the region sufficiently far away from the fuel

pool. Mathematically, the similarity solution is asymptotically correct in the far field, where the effects of the bottom boundary conditions are negligible. Such similarity solution was proposed by Klimenko and William [18] to derive the flame height for the circulation-controlled firewhirl with a strong vortex model, and therefore to remedy the divergence of axial velocity in the power-law vortex model. By following similar approach, Yu and Zhang [20] derived an analytical expression for the effective power exponent (i.e. $\alpha_{v,\mathrm{eff}}$) for their piecewise power-law vortex model.

Considering that the Lewis-number-weighted-species-species coupling function is of no mathematical advantages for arbitrary Lewis numbers, we can resort to the mixture fraction formulation with distinct transport properties in the fuel and oxidizer regions as

$$\tilde{\rho}\tilde{u}\frac{\partial Z}{\partial \tilde{x}}+\tilde{\rho}\tilde{v}\frac{\partial Z}{\partial \tilde{r}}-\alpha_Z\frac{2}{Pe}\frac{\partial}{\partial \tilde{x}}\left(\tilde{\rho}\widetilde{D}_F\frac{\partial Z}{\partial \tilde{x}}\right)-\alpha_Z\frac{2}{Pe}\frac{1}{\tilde{r}}\frac{\partial}{\partial \tilde{r}}\left(\tilde{\rho}\widetilde{D}_F\tilde{r}\frac{\partial Z}{\partial \tilde{r}}\right)=0 \tag{50}$$

where

$$Z=\frac{\tilde{Y}_F+\tilde{Y}_{O\infty}-\tilde{Y}_O}{\tilde{Y}_{F0}+\tilde{Y}_{O\infty}},\qquad \alpha_Z=\begin{cases}1, & Z>Z_{st}\\ Le_F/Le_O, & Z<Z_{st}\end{cases} \tag{51}$$

Here $Z>Z_{st}$ denotes the fuel region and $Z<Z_{st}$ the oxidizer region.

Applying the coordinate transformation (3) to Equation (51) and applying the large Peclet number approximation, we have

$$\hat{u}\frac{\partial Z}{\partial \xi}+\hat{v}\frac{\partial Z}{\partial \eta}-\alpha_Z\frac{1}{\eta}\frac{\partial}{\partial \eta}\left(\eta\frac{\partial Z}{\partial \eta}\right)=0 \tag{52}$$

The similarity solutions to the equation in the fuel and oxidizer regions are given in the piecewise form as

$$Z_F=\frac{1}{2\xi A}\exp\left(\int_0^\eta \hat{v}d\eta'\right),\qquad Z_O=\frac{Le_O}{Le_F}\frac{1}{2\xi A}\exp\left(\frac{Le_O}{Le_F}\int_0^\eta \hat{v}d\eta'\right) \tag{53}$$

where Z_F formally satisfies Equation (52) in the fuel region and Z_O in the oxidizer region. It has been recognized that the constant

$$A = \frac{1}{\xi}\int_0^{\infty} \hat{u} \exp\left(\int_0^{\eta} \hat{v} d\eta'\right) \eta d\eta \tag{54}$$

is actually the effective exponent $\alpha_{v,\text{eff}}$ to be determined in Appendix E [18, 23].

A composite solution of the mixture fraction, which is valid for the whole domain, can be formally written as a combination of Z_F and Z_O in the form of

$$Z = Z_O + c(\xi,\eta)(Z_F - Z_O) \tag{55}$$

where $c(\xi,\eta)$ is equal to unity inside the flame so that $Z = Z_F$, and to zero far away from the flame so that $Z = Z_O$. The magnitude of $c(\xi,\eta)$ is bounded in the interval of $[0,1]$ and the boundedness of the functions similar to $c(\xi,\eta)$ has been proved in the previous study [20]. The precise determination of $c(\xi,\eta)$ by numerically solving Equation (52) merits future studies but will not considered in the present study.

Equation (55) can be regarded as an approximate similarity solution, being valid far away from the fuel pool. The flame height can be determined by setting "radial" coordinate η equal to zero and the mixture fraction $Z = Z_{st}$, and Equation (55) is reduced to

$$\xi_h = \frac{Le_O}{Le_F}\frac{1}{2AZ_{st}}\left[1 + c(\xi_h,0)\left(\frac{Le_F}{Le_O} - 1\right)\right] \tag{56}$$

Applying the inverse transformation (3) to (56), we can obtain the flame height in physical coordinates as

$$\frac{x_h}{d_0} = \frac{Le_O}{Le_F}\frac{2}{A}\left(\frac{T_m}{T_0}\right)^{2-\alpha_T}\frac{Pe}{16Z_{st}}\left[1 + c(\xi_h,0)\left(\frac{Le_F}{Le_O} - 1\right)\right] \tag{57}$$

In spite of that $c(\xi_h,0)$ is not completely determined, we still can deduce some interesting results from Equation (57) as follows.

If Le_F and Le_O are arbitrary but their ratio is close to unity, namely, $Le_F/Le_O \approx 1$, the second term in the bracket of Equation (57) can be neglected and we have the flame height expression given

by

$$\frac{x_h}{d_0} = \frac{Le_O}{Le_F}\frac{2}{A}\left(\frac{T_m}{T_0}\right)^{2-\alpha_T}\frac{Pe}{16Z_{st}} \tag{58}$$

which accords with the leading-order solution of the flame height expression (47) except the factor A to be discussed below. Equation (58) verifies that the perturbation theory predicts the correct trend of the flame height dependence on the Lewis number ratio, and it also extends the validity of Equation (47) to the Lewis numbers substantially deviating from unity while their ratios are close to unity. Furthermore, we note that, $c(\xi_h, 0)$ takes the value of the function $c(\xi, \eta)$ at $\xi_h = O(1)$ and $\eta = 0$, corresponding to the farthest axial location of the flame at $x_h \sim d_0 O(Pe) \gg d_0$. In the present study, the order of magnitude of $c(\xi_h, 0)$ cannot be further determined, and hence the validity of Equation (58) cannot be extended to a more general situation of both arbitrary Lewis numbers and arbitrary Lewis number ratios, which certainly merits future studies with the help of numerical simulation.

Finally, the accordance of Equation (58) derived from the far-field similarity solution with Equation (47) from the perturbation theory implies that the role of A in Equation (58) must be equivalent to α_v in Equation (47). This provides an approach to determine the effective exponent α_v in the strong vortex model [18] and in the generalized power-law vortex model [20]. The details of the derivation are given in Appendix E.

6. Concluding remarks

A flame-sheet theory about the flame shape and height of circulation-controlled firewhirls has been established in the present study, with emphasis on the effects of differential diffusion, particularly of the non-unity and unequal Lewis numbers on the fuel and oxidizer sides of the flame sheet. By using the perturbation method and regarding the deviations of the fuel and oxidizer Lewis numbers from unity as small parameters, we obtained the series solutions of the Burke-Schumann-like transport equation for the Lewis-number-weighted coupling functions.

Subsequently, we extended the theory to arbitrary Lewis numbers by seeking the far-field similarity solutions for the mixture fraction in lieu of the coupling functions, which are of disadvantage under the general situation. By means of the mathematically rigorous series solutions, which are however limited to near-unity Lewis numbers, and the far-field similarity solutions for arbitrary Lewis numbers, which are however mathematically approximate, we fulfilled the objectives that motivated the present study as follows.

First, the leading-order series solutions yields a unified expression for dimensionless flame height, which can degenerate to the results obtained in the previous studies [19, 20]. The expression consists of four multiplicative factors accounting for the effects of various independent mechanisms as

$$\frac{x_h}{d_0} = \frac{Le_O}{Le_F}\frac{2}{\alpha_v}\left(\frac{T_m^{(0)}}{T_0}\right)^{2-\alpha_T}\frac{Pe}{16Z_{st}}$$

where the factor $Pe/16Z_{st}$ was first identified by Chuah *et al*. [3] for the Peclet number effect, the factor $2/\alpha_v$ by Klimenko and William [18] for the strong vortex effect, the factor $\left(T_m^{(0)}/T_0\right)^{2-\alpha_T}$ by Yu and Zhang [19] for the effects of variable, temperature-dependent density and mass diffusivity, and the factor Le_O/Le_F for the non-equal Lewis number effect. The Lewis number ratio, Le_O/Le_F, is found to be equal to D_F/D_O and consequently verifies that the mass-diffusivity-ratio model correction very recently proposed by Yu and Zhang [20] is the leading-order effect of differential diffusion.

Second, retaining the first-order series solutions in the perturbation theory yield an accurate albeit implicit expression and an approximate albeit explicit expression for the flame shape of the firewhirls for different Lewis numbers. The approximate flame shapes agree well with the accurate ones at the locations sufficiently away from the fuel pool, where the asymptotic expansion for large axial coordinate is valid. Both flame shape expressions indicate that a smaller fuel Lewis number, implying a larger fuel mass diffusivity for diffusional transport, tends to "slim" the flame shape in the axial direction and hence to enhance the flame height, whereas a smaller oxidizer Lewis numbers results in a stouter flame shape because the larger oxidizer mass diffusivity helps the oxidizer

transport to lower altitude.

Third, the flame shape expressions also suggest that, although the flame shape changes with the fuel and oxidizer Lewis numbers, the flame height changes slightly if the Lewis number ratio is fixed. This can be understood by that, for larger Lewis numbers, the mass diffusivities of fuel and oxidizer are both smaller so that the flame shape tends to be controlled by the axial convection because of the large Peclet number, and thus to be slimmer. For the same reason, smaller Lewis numbers will result in stouter flame shape because of the larger mass diffusion to all the directions.

Finally, the approximate far-field similarity solutions for the mixture fraction yield an alternative expression for flame height but for arbitrary Lewis numbers as

$$\frac{x_h}{d_0} = \frac{Le_O}{Le_F}\frac{2}{A}\left(\frac{T_m}{T_0}\right)^{2-\alpha_T}\frac{Pe}{16Z_{st}}\left[1 + c(\xi_h, 0)\left(\frac{Le_F}{Le_O} - 1\right)\right]$$

where the constant A is physically equivalent to α_v accounting for the strong vortex effect. Under the situation that the Lewis number ratio is close to unity, this expression is identical to that derived from the perturbation theory, verifying and extending the validity of the latter to Lewis numbers substantially deviating from unity. Further discussion on the effects of Lewis numbers in the most general situation requires the precise determination of $c(\xi_h, 0)$, by using numerical simulation, which merits future studies.

Acknowledgement

This work was supported by the Hong Kong RGC/GRF (operating under contract numbers PolyU 152217/14E and 152651/16E) and partly by the Hong Kong Polytechnic University (G-UA2M and G-YBGA).

Appendix A. "Closure Problem" of Firewhirls

To determine the boundary values T_0 and Y_{F0}, we must analyze the physics of the Stefan flow in the evaporation layer on the fuel pool surface. The evaporated fuel is both convectively and diffusively transported to feed the flame, where heat is generated and conducted to the evaporation layer to drive the Stefan flow. For mathematical simplicity, all the variables in Appendix A, $Q = \rho, u, Y_F, Y_O, T, p$, denote their functions $Q(r, x = 0)$, since the evaporation layer is located at $(x = 0, r < r_0)$.

Because the radial dimension of the evaporation layer is considerably larger than its axial dimension, the radial diffusion and convection is negligible compared with the dominant convection and diffusion in the axial direction. Consequently, integrating the conservation equation for the fuel mass fraction in the axial direction and recognizing that the total mass flux, ρu, is completely attributed to the evaporation of fuel (the inert gas and products are non-condensable), we have

$$\rho u Y_F - \rho D_F \frac{\partial Y_F}{\partial x} = \rho u \tag{A1}$$

According to the flame-sheet approximation, no oxidizer exists on the fuel side and its mass fraction vanishes as

$$Y_O = 0 \tag{A2}$$

Similarly, integrating the conservation equation for the enthalpy and recognizing that the net enthalpy flux, $\rho u c_p (T - T_0)$, is equal to the heat conduction flux, $\lambda \, \partial T / \partial x$, subtracted by the amount of heat required by evaporation, $\rho u q_v$, we have

$$\rho u c_p (T - T_0) - \lambda \frac{\partial T}{\partial x} = -\rho u q_v \tag{A3}$$

Solving Y_F and T from Equations (A1) and (A3) requires the determination of the axial velocity, u, and the density, ρ. The velocity and density are related by the body-force-free Bernoulli's equation

$$\int_{\infty}^{r} \frac{dp}{\rho} + \frac{1}{2} \rho (u^2 + v^2 + w^2) = 0 \tag{A4}$$

where the radial and angular velocities, v and w, are given for a given vortex model. The equation of state gives an additional relation between the density and the pressure of the gas mixture,

$$\rho = \frac{p}{RT} \tag{A5}$$

where the pressure is related to the fuel mass fraction and the temperature by the Clausius-Clapeyron relation

$$\frac{Y_F/W_F}{Y_F/W_F + (1-Y_F)/W_N} = \frac{p_\infty}{p}\exp\left[\frac{q_v}{R^o}\left(\frac{1}{T_{b,n}} - \frac{1}{T}\right)\right] \tag{A6}$$

where $T_{b,n}$ is the boiling point temperature at p_∞, W_F and W_N are the molecular weight of the fuel and the inert gas. Completely solving the above six coupled equations, (A1)-(A6), we can determine the six variables ρ, u, Y_F, Y_O, T, p, and therefore the problem is closed. It should be further clarified that the Dirichlet boundary conditions BC(3a) are based on the solutions of the closure problem, and that they cannot be treated as the mathematical simplification of Equations (A1)-(A6). Such a specification of boundary condition on the evaporating fuel layer is similar to that adopted in the theory of droplet vaporization and combustion [24]. Consequently, the boundary conditions BC(iii) in Yu and Zhang [20] and BC(3a) in Yu and Zhang [20] are mathematically redundant because they intermingle the boundary conditions with the closure problem.

Appendix B. Derivations of Equations (4) and (5)

Applying the coordinate transformation (3) to Equations (1) and (2), we obtained the following equations in ξ and η coordinates,

$$\begin{aligned}\left(\hat{u}\frac{\partial}{\partial\xi} + \hat{v}\frac{\partial}{\partial\eta}\right)\left(\tilde{Y}_F + \tilde{T}\right) - \frac{4Le_F}{Pe^2\tilde{\rho}}\left(\frac{\partial}{\partial\xi} + h\frac{\partial}{\partial\eta}\right)\left[\tilde{\rho}^3\tilde{D}_F^2\left(\frac{\partial}{\partial\xi} + h\frac{\partial}{\partial\eta}\right)\right]\left(\frac{\tilde{Y}_F}{Le_F} + \tilde{T}\right)\\ - Le_F\left(\frac{2g}{Pe\tilde{\rho}\tilde{r}}\frac{\partial}{\partial\xi} + \frac{1}{\tilde{\rho}^2\tilde{D}_F\tilde{r}}\frac{\partial}{\partial\eta}\right)\left(\frac{2\tilde{\rho}^3\tilde{D}_F^2 g\tilde{r}}{Pe}\frac{\partial}{\partial\xi} + \tilde{\rho}^2\tilde{D}_F\tilde{r}\frac{\partial}{\partial\eta}\right)\left(\frac{\tilde{Y}_F}{Le_F} + \tilde{T}\right) = 0\end{aligned} \tag{B1}$$

$$\left(\hat{u}\frac{\partial}{\partial\xi}+\hat{v}\frac{\partial}{\partial\eta}\right)\left(\tilde{Y}_F-\tilde{Y}_O\right)-\frac{4Le_F}{Pe^2\tilde{\rho}}\left(\frac{\partial}{\partial\xi}+h\frac{\partial}{\partial\eta}\right)\left[\tilde{\rho}^3\widetilde{D}_F^2\left(\frac{\partial}{\partial\xi}+h\frac{\partial}{\partial\eta}\right)\right]\left(\frac{\tilde{Y}_F}{Le_F}-\frac{\tilde{Y}_O}{Le_O}\right)$$
$$-Le_F\left(\frac{2g}{Pe\tilde{\rho}\tilde{r}}\frac{\partial}{\partial\xi}+\frac{1}{\tilde{\rho}^2\widetilde{D}_F\tilde{r}}\frac{\partial}{\partial\eta}\right)\left(\frac{2\tilde{\rho}^3\widetilde{D}_F^2 g\tilde{r}}{Pe}\frac{\partial}{\partial\xi}+\tilde{\rho}^2\widetilde{D}_F\tilde{r}\frac{\partial}{\partial\eta}\right)\left(\frac{\tilde{Y}_F}{Le_F}-\frac{\tilde{Y}_O}{Le_O}\right) \quad \text{(B2)}$$
$$=0$$

where g and h are given by

$$g(\tilde{x},\tilde{r})=\frac{1}{\tilde{\rho}^2\widetilde{D}_F}\int_0^{\tilde{x}}\frac{\partial}{\partial\tilde{r}}\left(\tilde{\rho}^2\widetilde{D}_F\right)dx',\qquad h(\tilde{x},\tilde{r})=\frac{Pe}{2\tilde{\rho}^2\widetilde{D}_F}\int_0^{\tilde{r}}\frac{\partial\tilde{\rho}}{\partial\tilde{x}}dr' \quad \text{(B3)}$$

to account for the variations of density and mass diffusivity gradients in axial and radial directions. The non-dimensional velocity components in Equation (B1) and (B2) are written as

$$\hat{u}=2\tilde{u}+2g\tilde{v},\qquad \hat{v}=2h\tilde{u}+\frac{Pe}{\tilde{\rho}\widetilde{D}_F}\tilde{v} \quad \text{(B4)}$$

Neglecting all the terms of $O(Pe^{-1})$ and $O(Pe^{-2})$ in the above equations, we can readily obtain Equations (4) and (5). Here we have invoked an approximation that

$$\frac{\tilde{\rho}^2\widetilde{D}_F\tilde{r}}{\int_0^{\tilde{r}}\tilde{\rho}dr'}=C(\xi) \quad \text{(B5)}$$

is independent of the coordinate η. This is a weak version of the Chapman-Rubesin approximation [34], which further requires $C(\xi)$ being a constant.

As we have discussed in Introduction, the firewhirl with large Peclet number is substantially elongated along the axial direction because the strong axial convection is dominant over that in the radial direction. In addition, the axial coordinate being scaled by a factor of $2/Pe$ through the transformation (3) indicates that the nondimensional velocities $\hat{u}$ and $\hat{v}$ in the $\xi-\eta$ space should be of the same order of magnitude. Consequently, we can conclude from Equation (B4) that $h\sim O(1)$, $g\sim O(1)$, $\tilde{u}\sim O(1)$, and $\tilde{v}\sim O(Pe^{-1})$, which implies $u/u_0=O(1)$ and $v/u_0=O(Pe^{-1})$.

Appendix C. Verification of Green's Function (29)

Applying the partial differential operator (17) to the Green's function (29), we have

$$\begin{aligned}\hat{L}_{\chi,\zeta}G(\chi,\chi',\zeta,\zeta') &= \frac{\partial}{\partial\chi}G(\chi,\chi',\zeta,\zeta') - \frac{1}{\zeta}\frac{\partial}{\partial\zeta}\left(\zeta\frac{\partial}{\partial\zeta}\right)G(\chi,\chi',\zeta,\zeta') \\ &= \delta(\chi-\chi')\int_0^\infty \omega J_0(\omega\zeta')J_0(\omega\zeta)\exp[-\omega^2(\chi-\chi')]d\omega \\ &- H(\chi-\chi')\int_0^\infty \omega^3 J_0(\omega\zeta')J_0(\omega\zeta)\exp[-\omega^2(\chi-\chi')]d\omega \\ &- H(\chi-\chi')\int_0^\infty \omega J_0(\omega\zeta')\frac{1}{\zeta}\frac{d}{d\zeta}\left[\zeta\frac{d}{d\zeta}J_0(\omega\zeta)\right]\exp[-\omega^2(\chi-\chi')]d\omega\end{aligned} \tag{C1}$$

Using the known properties of Bessel function, we can calculate the derivative of J_0 with respect to ζ in Equation (C1) as

$$\frac{1}{\zeta}\frac{d}{d\zeta}\left[\zeta\frac{d}{d\zeta}J_0(\omega\zeta)\right] = -\frac{1}{\zeta}\frac{d}{d\zeta}[\omega\zeta J_1(\omega\zeta)] = -\omega^2\frac{1}{\omega\zeta}\frac{d}{d\omega\zeta}[\omega\zeta J_1(\omega\zeta)] = -\omega^2 J_0(\omega\zeta) \tag{C2}$$

Substitution of (C2) in (C1) leads to the cancellation of the second and third term and yields

$$\hat{L}_{\chi,\zeta}G(\chi,\chi',\zeta,\zeta') = \delta(\chi-\chi')\int_0^\infty \omega J_0(\omega\zeta')J_0(\omega\zeta)\exp[-\omega^2(\chi-\chi')]d\omega \tag{C3}$$

Apparently, the RHS of (C3) vanishes for $\chi \neq \chi'$. For $\chi = \chi'$, the RHS of equation (C3) reduces to [31]

$$\int_0^\infty \omega J_0(\omega\zeta')J_0(\omega\zeta)d\omega = \frac{1}{\zeta'}\delta(\zeta'-\zeta) \tag{C4}$$

to derive which the integral representation of delta function in terms of Bessel functions has been used [35]. Since the integral element is $\zeta' d\zeta' d\chi'$, which cancel out the factor of $1/\zeta'$ in (C4), the conventional double integration with respect to $\delta(\chi-\chi')$ and $\delta(\zeta-\zeta')$ is equal to unity. Therefore, we verified that the Green's function (29) satisfies Equation (24).

Appendix D. Evaluation of I_F and I_D

Assuming that the four-fold integrations over distinct variables can be interchanged, we can rewrite I_F in the form of

$$I_F = \int_0^{\chi_f} H(\chi-\chi')\exp[-Le_F\omega^2(\chi-\chi')]\exp(-Le_F\varpi^2\chi')\,d\chi' \int_0^{\infty}\varpi^2 J_1(\varpi)d\varpi \times \int_0^{\infty}\omega J_0(\omega\zeta)d\omega\int_0^{\zeta_f} J_0(\omega\zeta')J_0(\varpi\zeta')\zeta' d\zeta' \tag{D1}$$

The integration over ζ' from 0 to ζ_f can be explicitly expressed by

$$I_F = \int_0^{\chi_f} H(\chi-\chi')\exp[-Le_F\omega^2(\chi-\chi')]\exp(-Le_F\varpi^2\chi')\,d\chi' \int_0^{\infty}\varpi^2 J_1(\varpi)d\varpi \times \int_0^{\infty}\frac{\zeta_f}{\omega^2-\varpi^2}\left[\omega J_0(\varpi\zeta_f)J_1(\omega\zeta_f)-\varpi J_0(\omega\zeta_f)J_1(\varpi\zeta_f)\right]\omega J_0(\omega\zeta)d\omega \tag{D2}$$

For small ζ_f, which physically corresponds to the flame sufficiently away from the fuel pool, we can expand the Bessel functions in Taylor series, keep the terms of $O(\zeta_f)$, and have

$$\omega J_0(\varpi\zeta_f)J_1(\omega\zeta_f)-\varpi J_0(\omega\zeta_f)J_1(\varpi\zeta_f) \approx \omega\frac{1}{2}\omega\zeta_f-\varpi\frac{1}{2}\varpi\zeta_f=\frac{1}{2}\zeta_f(\omega^2-\varpi^2) \tag{D3}$$

Substituting (D3) into (D2), we have

$$I_F = \frac{1}{2}\zeta_f^2\int_0^{\chi_f} H(\chi-\chi')d\chi'\int_0^{\infty}\omega J_0(\omega\zeta)\exp[-Le_F\omega^2(\chi-\chi')]\,d\omega \times \int_0^{\infty}\varpi^2 J_1(\varpi)\exp(-Le_F\varpi^2\chi')\,d\varpi \tag{D4}$$

The integrations over ω and ϖ can be explicitly expressed and hence the above equation can be written by

$$I_F = \frac{\zeta_f^2}{16Le_F^3}\int_0^{\chi_f}\frac{H(\chi-\chi')}{(\chi-\chi')\chi'^2}\exp\left[-\frac{\chi+\chi'(\zeta^2-1)}{4Le_F\chi'(\chi-\chi')}\right]d\chi' \tag{D5}$$

which gives the simplified expression of I_F in the form of single-fold integration and is valid for small ζ_f.

To derive the simplified expression of I_O, we noted that the sum of I_F and I_O gives the integration over the whole domain,

$$I_O + I_F = \int_0^\infty \int_0^\infty H(\chi - \chi') \int_0^\infty \omega J_0(\omega\zeta') J_0(\omega\zeta) \exp[-Le_F \omega^2 (\chi - \chi')] d\omega \times \int_0^\infty \varpi^2 J_0(\varpi\zeta') J_1(\varpi) \exp(-Le_F \varpi^2 \chi') d\varpi \, \zeta' d\zeta' d\chi' \tag{D6}$$

This four-fold integral can be evaluated exactly as follows. By means of the interchangeability of the integrations over various variables, we can rewrite the integral as

$$I_O + I_F = \int_0^\infty H(\chi - \chi') \exp[-Le_F \omega^2 (\chi - \chi')] \exp(-Le_F \varpi^2 \chi') \, d\chi' \int_0^\infty J_0(\omega\zeta) d\omega \times \int_0^\infty \varpi^2 J_1(\varpi) d\varpi \int_0^\infty \omega J_0(\omega\zeta') J_0(\varpi\zeta') \zeta' d\zeta' \tag{D7}$$

Integrating (D7) over ζ' gives

$$I_O + I_F = \int_0^\infty H(\chi - \chi') \exp(-Le_F \varpi^2 \chi') \, d\chi' \int_0^\infty \varpi^2 J_1(\varpi) d\varpi \times \int_0^\infty \delta(\omega - \varpi) \exp[-Le_F \omega^2 (\chi - \chi')] J_0(\omega\zeta) d\omega \tag{D8}$$

Integrating (D8) over ω gives

$$I_O + I_F = \int_0^\infty H(\chi - \chi') d\chi' \int_0^\infty \exp(-Le_F \varpi^2 \chi) \, \varpi^2 J_1(\varpi) d\varpi \tag{D9}$$

Integrating (D9) over χ' gives

$$I_O + I_F = \chi \int_0^\infty \varpi^2 J_0(\varpi\zeta) J_1(\varpi) \exp[-Le_F \varpi^2 \chi] \, d\varpi \tag{D10}$$

Considering (D10) and (D5) together, we have

$$I_O = \chi \int_0^\infty \varpi^2 J_0(\varpi\zeta) J_1(\varpi) \exp[-Le_F \varpi^2 \chi] \, d\varpi - \frac{\zeta_f^2}{16 Le_F^3} \int_0^{\chi_f} \frac{H(\chi - \chi')}{(\chi - \chi') \chi'^2} \exp\left[-\frac{\chi + \chi'(\zeta^2 - 1)}{4 Le_F \chi' (\chi - \chi')} \right] d\chi' \tag{D11}$$

which gives the simplified expression of I_O in the form of single-fold integration and is valid only for small ζ_f.

For the flame close to the fuel pool, namely $\chi = \chi_f = O(\epsilon)$, both integrals I_F and I_O are of order $O(\epsilon)$ as readily deduced from (D2) and (D10).

Appendix E. Determination of α_v

In Chuah *et al.*'s theory, the vortical flow is modelled by a Burgers vortex [3], whose stream function contains a second-order power function of the radial coordinate. To account for the stronger vortical flow of firewhirls, Klimenko and Williams proposed a power-law vortex containing a Burgers vortex core to eliminate the velocity singularity at the axis [18]. In the present study, the piecewise generalized power-law vortex model, which was proposed and discussed in detail by Yu and Zhang [20] in their recent theory, was adopted and is written in the form of

$$\psi = \begin{cases} s(\xi)\eta^{\alpha_{v1}}, & \eta < \eta_c \\ \eta_c^{\alpha_{v1}-\alpha_{v2}} s(\xi)\eta^{\alpha_{v2}}, & \eta \geq \eta_c \end{cases} \tag{E1}$$

where η_c is the inner core radius, and $s(\xi)$ is to be determined by conservation laws and boundary conditions. The exponent $\alpha_{v1} > 2$ characterizes the flow within the vortex core, and $\alpha_{v2} < 2$ accounts for the deviation of the vortical flow from the Burgers vortex.

Differentiating (E1) with respect to η and ξ, we have the velocity components given by

$$\hat{u} = \begin{cases} \alpha_{v1}\eta^{\alpha_{v1}-2} s(\xi), & \eta < \eta_c \\ \alpha_{v2}\eta_c^{\alpha_{v1}-\alpha_{v2}} s(\xi)\eta^{\alpha_v-2}, & \eta \geq \eta_c \end{cases} \tag{E2}$$

$$\hat{v} = \begin{cases} -s'(\xi)\eta^{\alpha_{v1}-1}, & \eta < \eta_c \\ -\eta_c^{\alpha_{v1}-\alpha_{v2}} s'(\xi)\eta^{\alpha_{v2}-1}, & \eta \geq \eta_c \end{cases} \tag{E3}$$

By transforming $\hat{u}$ and $\hat{v}$ back to the physical coordinates, we can verify that the velocity field satisfies the continuity equation [20], indicating that the power-law vortex in the ξ-η space is physically reasonable.

Comparing the flame height derived from the far-field similarity solution, Equation (57), to that from the perturbation solution, Equation (47), we can conclude that the constant A plays the same role as the exponent of the generalized power-law vortex model, and thus we have

$$\alpha_v = A = \frac{1}{\xi}\int_0^{\infty} \hat{u} \exp\left(\int_0^{\eta} \hat{v} d\eta'\right) \eta d\eta \tag{E4}$$

By using the velocity components in (E2) and (E3), we can analytically determine the exponent in the form of

$$\alpha_v = \alpha_{v1} - (\alpha_{v1} - \alpha_{v2}) \exp\left(-\frac{\eta_c^{\alpha_{v1}}}{\alpha_{v1}}\right) \tag{E5}$$

which is identical to that given by Yu and Zhang [20]. Further determination of the precise value of α_v requires experimental data for velocity measurement of firewhirls, which are currently unavailable in literature. Klimenko and William suggested $1.33 < \alpha_v < 1.43$ according to their constant-density strong vortex model with a compensating regime.

References

[1] H.W.Y. Emmons, Shuh-Jing. The fire whirl. Symposium (International) on Combustion; 1967. p. 475-488.

[2] K. Kuwana, K. Sekimoto, K. Saito, F.A. Williams, Scaling fire whirls, Fire Safety Journal 43 (2008) 252-257.

[3] K.H. Chuah, K. Kuwana, K. Saito, F.A. Williams, Inclined fire whirls, P Combust Inst 33 (2011) 2417-2424.

[4] J.A. Lei, N.A. Liu, L.H. Zhang, H.X. Chen, L.F. Shu, P. Chen, Z.H. Deng, J.P. Zhu, K. Satoh, J.L. de Ris, Experimental research on combustion dynamics of medium-scale fire whirl, P Combust Inst 33 (2011) 2407-2415.

[5] J. Lei, N.A. Liu, L.H. Zhang, K. Satoh, Temperature, velocity and air entrainment of fire whirl plume: A comprehensive experimental investigation, Combustion and Flame 162 (2015) 745-758.

[6] F. Battaglia, K.B. McGrattan, R.G. Rehm, H.R. Baum, Simulating fire whirls, Combustion Theory and Modelling 4 (2000) 123-138.

[7] F. Battaglia, R.G. Rehm, H.R. Baum, The fluid mechanics of fire whirls: An inviscid model, Physics of Fluids 12 (2000) 2859-2867.

[8] K.H. Chuah, G. Kushida, The prediction of flame heights and flame shapes of small fire whirls, P Combust Inst 31

(2007) 2599-2606.

[9] K. Kuwana, K. Sekimoto, K. Saio, F.A. Williams, Y. Hayashi, H. Masuda, Can we predict the occurrence of extreme fire whirls?, Aiaa J 45 (2007) 16-19.

[10] R. Zhou, Z.N. Wu, Fire whirls due to surrounding flame sources and the influence of the rotation speed on the flame height, J Fluid Mech 583 (2007) 313-345.

[11] K.H. Chuah, K. Kuwana, K. Saito, Modeling a fire whirl generated over a 5-cm-diameter methanol pool fire, Combustion and Flame 156 (2009) 1828-1833.

[12] K. Kuwana, S. Morishita, R. Dobashi, K.H. Chuah, K. Saito, The burning rate's effect on the flame length of weak fire whirls, P Combust Inst 33 (2011) 2425-2432.

[13] K. Zhou, N. Liu, K. Satoh, Experimental research on burning rate, vertical velocity and radiation of medium-scale fire whirls, Fire Safety Science 10 (2011) 681-691.

[14] Y. Hayashi, K. Kuwana, T. Mogi, R. Dobashi, Influence of Vortex Parameters on the Flame Height of a Weak Fire Whirl via Heat Feedback Mechanism, Journal of Chemical Engineering of Japan 46 (2013) 689-694.

[15] K. Kuwana, K. Sekimoto, T. Minami, T. Tashiro, K. Saito, Scale-model experiments of moving fire whirl over a line fire, P Combust Inst 34 (2013) 2625-2631.

[16] K. Zhou, N. Liu, L. Zhang, K. Satoh, Thermal radiation from fire whirls: revised solid flame model, Fire Technology 50 (2014) 1573-1587.

[17] J. Lei, N. Liu, K. Satoh, Buoyant pool fires under imposed circulations before the formation of fire whirls, P Combust Inst 35 (2015) 2503-2510.

[18] A.Y. Klimenko, F.A. Williams, On the flame length in firewhirls with strong vorticity, Combustion and Flame 160 (2013) 335-339.

[19] D. Yu, P. Zhang, On the flame heigth of circulation-controlled firewhirls with variable density, P Combust Inst 36 (2017) 3097-3104.

[20] D. Yu, P. Zhang, On flame height of circulation-controlled firewhirls with variable physical properties and in power-law vortices: A mass-diffusivity-ratio model correction, Combustion and Flame 182 (2017) 36-47.

[21] C. Fire, California Fire Siege 2007: An Overview, 2008.

[22] S. Soma, K. Saito, Reconstruction of fire whirls using scale models, Combustion and Flame 86 (1991) 269-284.

[23] A.Y. Klimenko, Strong swirl approximation and intensive vortices in the atmosphere, J Fluid Mech 738 (2014) 268-298.

[24] C.K. Law, Combustion Physics, Cambridge University Press, 2006.

[25] F.A. Williams, Combustion Theory 2ed., The Benjamin/Cummings, 1985.

[26] C.K. Law, Recent Advances in Droplet Vaporization and Combustion, Prog Energ Combust 8 (1982) 171-201.

[27] C.K. Law, H.K. Law, A D2-Law for Multicomponent Droplet Vaporization and Combustion, Aiaa J 20 (1982) 522-527.

[28] A. Liñán, M. Vera, A.L. Sánchez, Ignition, liftoff, and extinction of gaseous diffusion flames, Annual Review of Fluid Mechanics 47 (2015) 293-314.

[29] P.M. Chung, Chemically reacting nonequilibrium boundary layers, Advances in heat transfer 2 (1965) 109-270.

[30] S.H. Chung, C.K. Law, Burke-Schumann Flame with Streamwise and Preferential Diffusion, Combust Sci Technol 37 (1984) 21-46.

[31] S. Hassani, Mathematical Physics: A Modern Introduction to Its Foundations, 2 ed., Springer International Publishing, 2013.

[32] A.H. Nayfeh, Introduction to perturbation techniques, John Wiley & Sons, 2011.

[33] A.Y. Klimenko, Moderately strong vorticity in a bathtub-type flow, Theoretical and Computational Fluid Dynamics 14 (2001) 243-257.

[34] N. Peters, Turbulent Combustion, Cambridge University Press, 2000.

[35] NIST Handbook of Mathematical Functions, National Institute of Standards and Technology Cambridge University Press, 2010.

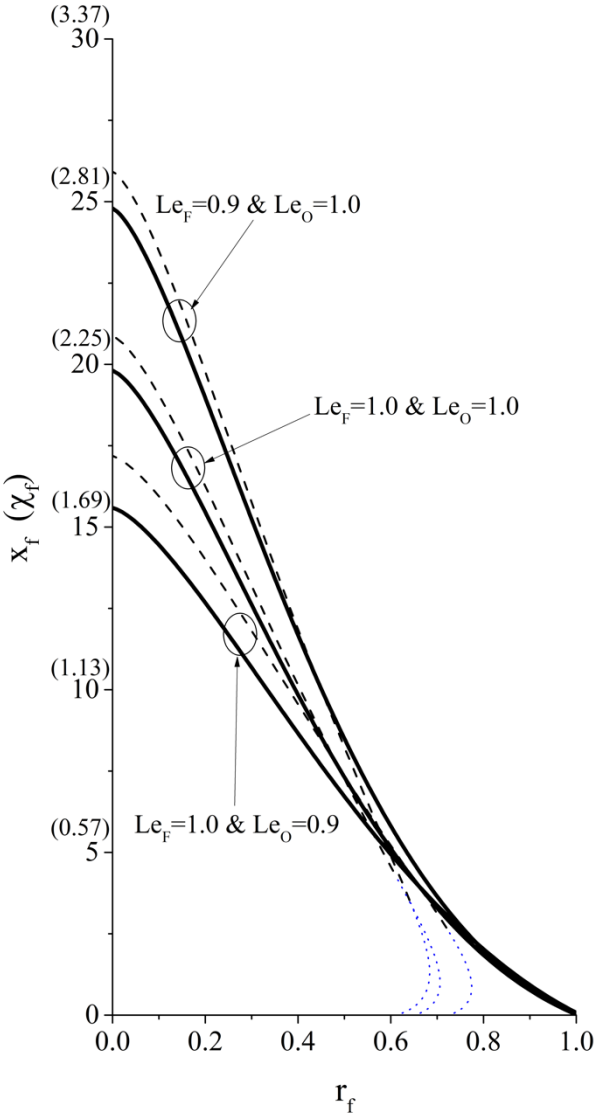

Figure 1. Approximate flame shapes at different Lewis numbers. The solid curves represent the results from Equation (39), which is the exact, implicit solution of flame shape. The dashed curves represent the results from Equation (44), which the approximate, explicit solution of flame shape. The dotted curves indicate that the extension of Equation (44) to the region close to liquid pool will cause physically unrealistic turning points.

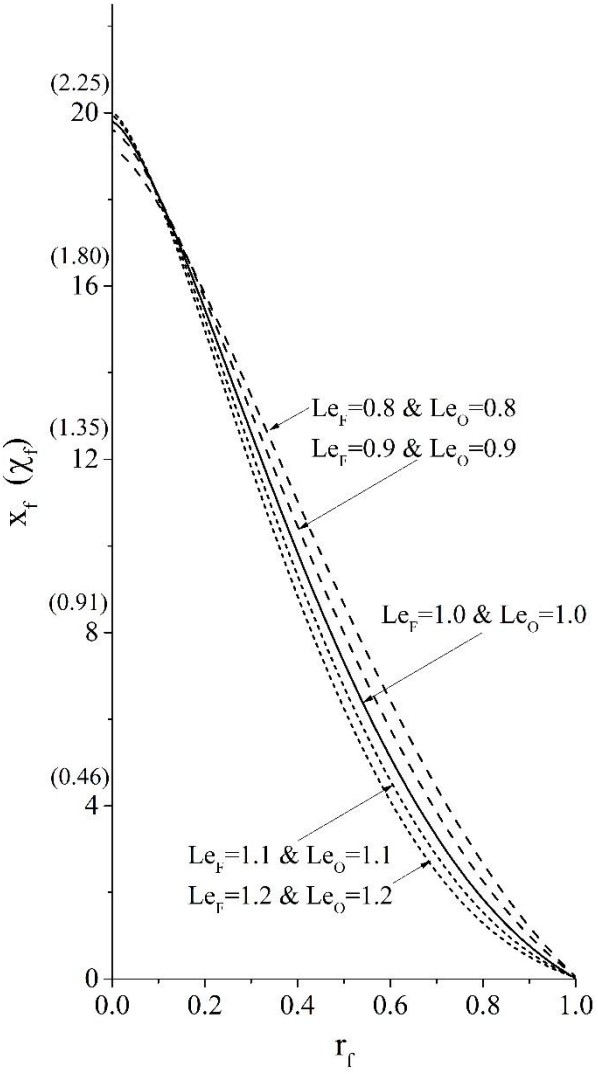

Figure 2. Effects of equal but non-unity Lewis numbers on the flame shape.